DISCLAIMER

This report was prepared as an account of work sponsored by an agency of the United States Government. Neither the United States Government nor any agency thereof, nor any of their employees, makes any warranty, express or implied, or assumes any legal liability or responsibility for the accuracy, completeness, or usefulness of any information, apparatus, product, or process disclosed, or represents that its use would not infringe privately owned rights. Reference herein to any specific commercial product, process, or service by trade name, trademark, manufacturer, or otherwise does not necessarily constitute or imply its endorsement, recommendation, or favoring by the United States Government or any agency thereof. The views and opinions of authors expressed herein do not necessarily state or reflect those of the United States Government or any agency thereof. Reference herein to any social initiative (including but not limited to Diversity, Equity, and Inclusion (DEI); Community Benefits Plans (CBP); Justice 40; etc.) is made by the Author independent of any current requirement by the United States Government and does not constitute or imply endorsement, recommendation, or support by the United States Government or any agency thereof.

SANDIA REPORT
SAND2025-12503
Printed October 2025

Sandia National Laboratories

Measurement of Close-in Ground Motion from an Underground Chemical Explosion

Richard E. Robey, Andrew A. Wright, Alfred H. Cochrane and the PE1 Experiment Team[1]

1: See acknowledgements and doi: 10.2172/2345984

Prepared by
Sandia National Laboratories
Albuquerque, New Mexico
87185 and Livermore,
California 94550

Issued by Sandia National Laboratories, operated for the United States Department of Energy by National Technology & Engineering Solutions of Sandia, LLC.

Available to DOE and DOE contractors from
U.S. Department of Energy
Office of Scientific and Technical Information
P.O. Box 62
Oak Ridge, TN 37831

Telephone: (865) 576-8401
Facsimile: (865) 576-5728
E-Mail: reports@osti.gov
Online ordering: http://www.osti.gov/scitech

Available to the public from
U.S. Department of Commerce
National Technical Information Service
5301 Shawnee Rd
Alexandria, VA 22312

Telephone: (800) 553-6847
Facsimile: (703) 605-6900
E-Mail: orders@ntis.gov
Online order: https://classic.ntis.gov/help/order-methods/

ACKNOWLEDGEMENTS

This Low Yield Nuclear Monitoring (LYNM) research was funded by the National Nuclear Security Administration, Defense Nuclear Nonproliferation Research and Development (NNSA DNN R&D). The authors acknowledge important interdisciplinary collaboration with scientists and engineers from LANL, LLNL, NNSS, PNNL, and SNL.

The authors wish to acknowledge the National Nuclear Security Administration Office of Defense Nuclear Nonproliferation for funding this research. We also greatly appreciate the support provided by the Pacific Northwest National Laboratory team including Hunter Knox, Chris Strickland, Carolyn Seifert, and Jeff Burghardt; field support from our colleagues at MSTS including Damien D'Sant Angelo and George Salyer; guidance from our Lawrence Livermore colleagues Elizabeth Dzenitis and Sean Ford; as well as guidance and support from our colleagues at Sandia National Laboratories, including Scott Broome, Joseph Pope, Manny Montano, Taylor Myers, Giorgia Bettin, Marc Williams, Stephanie Teich-McGoldrick, and Jose Falliner. We are very grateful to Avery (Zack) Cashion for his invaluable technical excellence, advisement, and contributions to SPE and DAG campaigns that paved the way for this work as well as Jiann Su for the earlier campaign execution and PE1 in-tunnel shock mounting. We additionally thank Jacquline Weeks for technical editing expertise.

Sandia National Laboratories is a multi-mission laboratory managed and operated by National Technology and Engineering Solutions of Sandia, LLC., a wholly owned subsidiary of Honeywell International, Inc., for the U.S. Department of Energy's National Nuclear Security Administration under contract DE-NA0003525.

CONTENTS

1. Introduction 8
2. System Design 10
   2.1. Sensor Modules 10
   2.2. Near-Source Accelerometer Module 10
   2.3. Drift Accelerometer Module 11
   2.4. Prototype Accelerometer Module 11
   2.5. Accelerometer Module Data Cables 12
   2.6. Data Acquisition Facility 13
3. Installation and Emplacement 15
4. Insitu Performance 18
   4.1. Noise Assessment 18
   4.2. Dynamic Response Testing 18
   4.3. Experiment Performance 19
5. Conclusions 21

LIST OF FIGURES

Figure 1-1. Geographic and geologic setting 9
Figure 2-1. Near-source accelerometer module 10
Figure 2-2. Near-source Accelerometer Prototype 4 kilo-g response 12
Figure 2-3. Expected frequency response of drift and near-source cables 13
Figure 2-4. Accelerometer DAQ enclosure w/ shock isolators 14
Figure 3-1. P-Tunnel infrastructure and experiment locations 15
Figure 3-2. Instrument borehole locations 15
Figure 3-3. Typical: Instruments emplaced in drift vaults and rib collars 16
Figure 4-1. Initial drift accelerometer noise assessment; 18
Figure 4-2. AWD drift accelerometer response 19
Figure 4-3. Raw waveform from near-source and drift accelerometers 19
Figure 4-4. Radial waveform from drift accelerometers 20

LIST OF TABLES

Table 2-1. Sensor and Cable Parameters 13
Table 2-2. DAQ and System Sensitivity 14
Table 3-1. Emplaced Instrument Locations and Source Range 17

EXECUTIVE SUMMARY

Understanding the geophysical response near an underground explosion is crucial for generating insights into the source and emplacement conditions that produce distinct observations in monitoring scenarios occurring at greater distances. Recently, Shot A of the Low Yield Nuclear Monitoring (LYNM) Physics Experiment 1 (PE1) series was conducted at the Nevada National Security Site to provide ground truth for subsurface explosion signal models. This experiment resulted in measuring near-source ground motion at distances ranging from 70 to 1000 m/kt with a 99% success rate, yielding high-fidelity knowledge of the near-field response that can serve as benchmarks for future numerical modeling and experiment planning. However, technical challenges exist in observing near-source phenomena while safeguarding sensitive data acquisition components from the detrimental effects of ground motion in the subsurface. This report outlines tools and techniques to address challenges associated with observing near-source accelerations and within the tunnel drift of the PE1 test bed. Additionally, we describe key systems designed with both modern advancements and legacy guidance to maximize the collection of high-quality ground motion data, which may be applied to constitutive and computational models, leading to new or improved understanding of the near- and far-field signals produced by underground explosions.

ACRONYMS AND DEFINITIONS

Acronym/Term	Definition
AWD	Accelerated weight drop
DAG	Dry Alluvium Geology
DAQ	Data acquisition system
HE	High explosive
GZ	Ground zero
IDAQ	Integrated data acquisition system
IMU	Inertial measurement unit
NS	Near-source
PE1	Physics Experiment
PI	Pacific Instruments
PNNL	Pacific Northwest National Laboratory
SDG	Stanford Delay Generator
SPE	Source Physics Experiment
UGT	Underground test

1. INTRODUCTION

The Physics Experiment 1 series consists of three planned chemical explosive experiments hosted in Area 12 of the Nevada National Security Site (NNSS) within the Aqueduct Mesa (Myers, 2024). The campaign utilized an underground complex known as P-Tunnel (U12.P). The first experiment, known as PE1-A, was structured around complex sensor networks, ranging from prompt measurements taken within the explosive cavity, to atmospheric measurements taken at distances more than 5 km. The range of deployed sensors are designed to capture the full scope of subsurface explosion phenomena, including both near-field and far-field measurements.

Near-field measurements (sometimes called free-field) are taken from within the native geology, with minimal boundary discontinuities that might exist in the complex subterranean environments. Near-field monitoring instruments are designed to withstand significant loading in response to bulk ground motion, which is well-coupled to the instrument. Near-source measurements (a subset of near-field) are subject to high amplitude loading by virtue of their small stand-off distances, the instrument packages must be able to capture complex ground motion as explosive energy causes material compaction and transmission of a strong local ground shock. In contrast, *far-field* measurements are taken at greater standoff distances from the explosion relative to the near-field, these may include shallowly buried instruments outside of a tunnel complex or permanent monitoring stations. Instrument stations considered far-field could range from 100's of meters to 10's of km in distance from the surface location of a ground zero (GZ) depending on source size.

Together, these measurements of the ground motion enhance our understanding of the *interplay between an energetic source and unique geology*, which is vital for global monitoring as it helps to interpret far-field signals more accurately. A significant number of UGTs have been conducted at the NNSS in three geologies: granite, alluvium and tuff. These silicate rocks demonstrate distinctive deformation, attenuation, and transmission responses to explosive insult. Granite is the strongest mechanically, having minimal pore volume resulting in the highest density and therefore compressional wave velocities. Alluvium is on the opposite end of the mechanical spectrum from granite, consisting of settled detritus from nearby tuff and carbonate rock mountains at the NNSS. Ground motion in granite and dry alluvium was studied during the Source Physics Experiment (SPE) Phase 1 and Phase 2 (also known as the Dry Alluvium Geology (DAG) series) with chemical explosive yields in tons TNT equivalent (Townsend, 2019 and Larotonda, 2021). Both SPE Phase 1 and DAG prioritized near-source ground motion, creating opportunities to understand low yield chemical explosives as nuclear surrogates (Rougier, 2015) and correlate diagnostics not previously used in ground motion studies (Mellors, 2021).

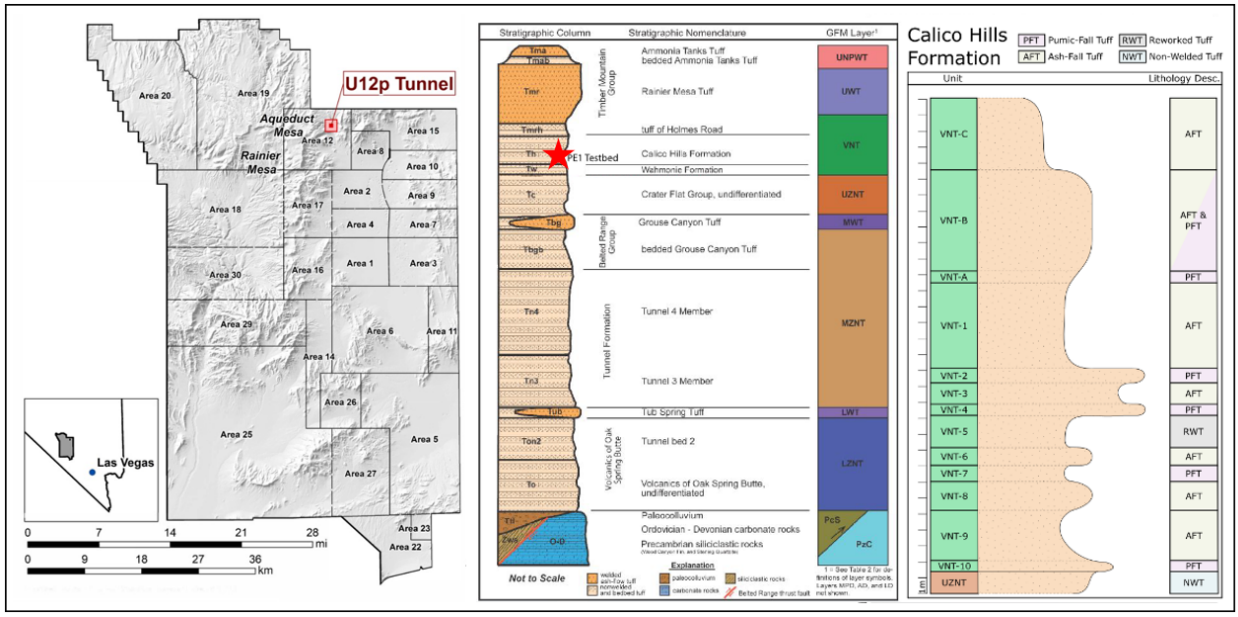

Figure 1-1. Geographic and geologic setting
NNSS site map (left), Area 12 stratigraphic column (center) and detailed lithology (right)

In contrast, chemical surrogate experiments have not been conducted in tuff since the Non-Proliferation Experiment also known as the chemical kiloton (Denny,1994). The tuffaceous structures at the NNSS consist of a variety of volcanic units which are overlayed on carbonates and siliclastic rock. The volcanic formation is substantially layered and consists of either non-welded or bedded tuffaceous members, depending on their degree of geologic alteration as shown in Figure 1-1 (Bodmer, 2024). The members may be further divided into sub-units based on subtle textural differences (compactable matrix or granular structure), degree of permeability, porosity, and a range of pore volume saturation, all of which affect the tuff's mechanical behavior. These properties influence dynamic compression behavior (Erskine, 1994) and have been empirically shown to change ground motion effects (Perret, 1974) and create potential variability in source to geology coupling across tunnel complexes (Fourney, 1994). Instrumentation boreholes in the present experiments were expected to span from Calico Hills sub-units VNT-C (vitric non welded tuff) to UZNT (upper zeolitic non welded tuff), so understanding the degree of geologic variability is critical to understand the source response into the formation and subsequent ground motion.

To elicit a response representative of a low-yield explosion, 2.8 m^3 of a chemical high explosive (HE), Composition B was detonated on October 18, 2023. During the explosion, approximately 16.3 tons of TNT-equivalent energy was released into a mined cavity that was backfilled with dry sand to create seismic coupling (Myers, 2024). Expected effects generated by the chemical explosion ranged from prompt ground motion to fractures driven into the formation by source gas and accompanying tracer material migration away from the cavity into the test bed. This was referred as experiment A, one of three chemical explosive experiments to be conducted under the PE1 experimental venture.

2. SYSTEM DESIGN

2.1. Sensor Modules

From a technical standpoint, the PE1 series has primarily focused on developing a high-fidelity test bed to better observe source and geology interactions. With the goal of maximizing our understanding of ground motion, we considered several existing explosion models designed to maximize near-field acceleration data (Ford, 2020). While substantial physics differences exist between chemical and nuclear sources, chemical sources can be estimated to be about twice as effective at creating ground motion in volcanic tuff (Goldstein, 1994). Prior to the PE1 mining activities, the effective acceleration (due to degree of saturation/mechanical properties where the source was to be emplaced) was not well known, but we anticipated a reasonable range of accelerations below 1 kilo-g, at scaled ranges from about 70 to 1000 $m/kt^{1/3}$ (Ford, 2020). To capture this data, we selected a series of gauge ranges from existing off-the-shelf integrated electronics piezo-electric (IEPE) sensors, which use bias voltage calibrated linearly to the measurement of interest. Because the accelerometer data acquisition system (DAQ) must be located as far away from the experiment as possible to minimize ground shock to sensitive acquisition electronics, utilization of long cables is critical in near-field explosive measurements; IEPE sensors are advantageous in this context because, when they are powered with greater driving currents, they are capable of propagating measurement signals to greater distances with improved signal-to-noise ratios.

To properly emplace and grout the sensors into a series of P-tunnel boreholes, the IEPE sensors were packaged into aluminum modules and potted in place with non-conductive epoxy (in a manner similar to legacy ground motion instruments) (Smith, 1996). Different levels of ground motion were expected in the two different borehole positions, so two different module styles were required: *near-source* and *drift*.

The basic module designs differed based on expected measurement range which was driven by their installation location and complexity relative to the chemical explosive source. The *near-source* modules were conveyed through the tunnel wall or rib into boreholes with locations above, below and to the side of GZ thus creating opportunity for very close-in measurements (10's of meters distance). *Drift* accelerometers were installed in vertical boreholes in the mine floor or invert at much greater distances from GZ (100's of meters) with lower amplitude expectations and aptly named for their location in the mined tunnel or drift.

2.2. Near-Source Accelerometer Module

The five *near-source modules* (Figure 2-1), were to include PCB Corporation +/-5 kilo-g IEPE accelerometers, residing at scaled ranges from 70 to 450 $m/kt^{1/3}$. To create measurement redundancy, two matching orthogonal sets of single-axis sensors were designed into each module body. To assess electromagnetic noise that could be caused by inductance of firing cables, detonation of the chemical explosive, or even tunnel infrastructure, a placebo sensor with an unstressed piezoelectric crystal was also included as a reference channel.

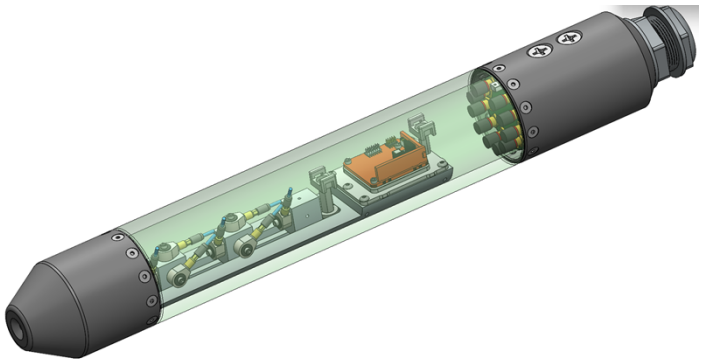

Figure 2-1. Near-source accelerometer module

These modules were emplaced in three relatively deep near-source instrumentation boreholes had length-to-diameter (L/D) ratios exceeding 400 and were planned at sub (45° below), super (45° above) and near horizontal inclinations as discussed further in Section 3. The blind installation of the near-source modules was planned on semi-rigid PVC pipe. While the emplaced module locations were planned to effectively evaluate the motion generated by the source; the local azimuthal orientation of the module within the borehole was to be measured with a Xsens inertial measurement unit (IMU) with an attitude and heading reference system (including an independent set of gyroscopes, accelerometers, and magnetometers) integrated into each module. The inertial measurements were also designed to align the local sensor axis to the source cavity and allow us to evaluate corrections to the primary accelerometer measurements using the roll about the axis of the module caused by spurious pipe rotation or helical buckling of the conveyance pipe during installation.

2.3. Drift Accelerometer Module

The seven *drift modules* utilized lower-range 50 g Dytran Corporation sensors and 500 g PCB Corporation sensors designed to take measurements in scaled ranges from about 180 to 1000 $m/kt^{1/3}$. The drift modules were emplaced and grouted into relatively shallow boreholes with L/D ratios < 100. Drift instrumentation boreholes were to be drilled vertically into the invert or floor of the U12p.06 drift tunnel as discussed further in Section 3. At these depths sensors modules were mechanically aligned (radially) to the source therefore IMUs were deemed unnecessary.

2.4. Prototype Accelerometer Module

To assess the survivability of the modules at shock levels near the top of the sensors' range, a prototype near-source module was constructed using relatively short cables, a National Instruments (NI) CompactDAQ Chassis, and several IEPE-compatible NI-9230 cards. To evaluate the modules' performance, the prototype was then subjected to a 4 kilo-g shock with a 10% pulse duration of about 0.9 ms. The resulting magnitude response (in dB) versus frequency (in Hz) is shown for the event duration in Figure 2-2. The top frame represents the longitudinal response to the shock down the axis of the cylinder (x- axis), which introduced significant modal oscillations in the orthogonal axes. The center and bottom frames show the shocks applied to the module in the radial and tangential directions, which introduced relatively little transverse signal. The sensors onboard the prototype module survived over 70 mechanical shocks ranging from 40 to 4 kilo-g's in the principal directions.

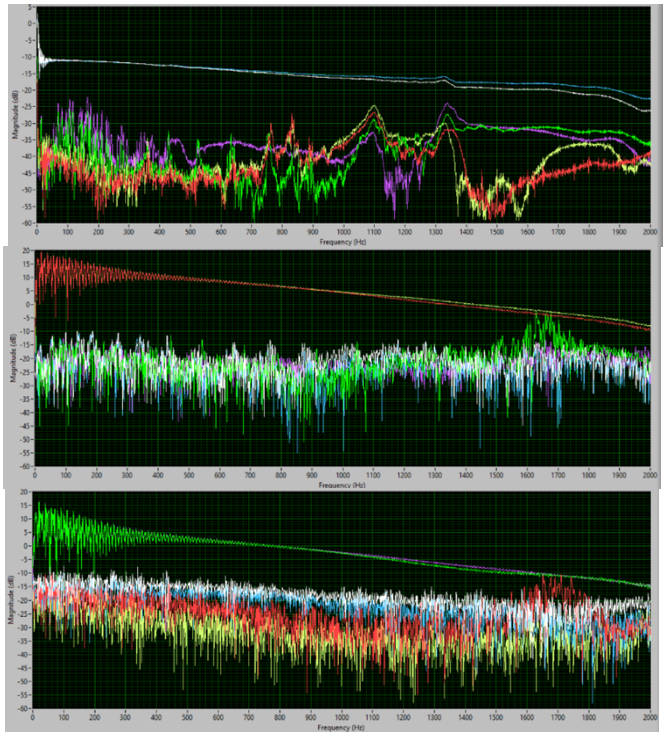

Figure 2-2. Near-source Module Prototype 4 kilo-g response
(axial direction, top; radial direction, center; transverse direction, bottom)

2.5. Accelerometer Module Data Cables

Long sensor *datalink* cables connected each of the near-field and drift modules to the accelerometer DAQ location nearer the mine entrance at the 650 infrastructure alcove. Short cable lengths were preferred, but lengths of < 1200 ft were required; to prevent excessive cable lengths from behaving as an undesirable low-pass filter, a signal conditioner was used to drive current to the sensors. The final cable design consisted of 12 pairs of stranded conductors that were both shielded and twisted to minimize the datalink's exposure from radio frequency and electro-magnetic interference distortion. Each datalink cable bundle was also shielded and included a drain wire. Frequency response of the installation's design was calculated as a function of driving current (which raises or lowers the maximum frequency response of the system), as governed by Equation (1):

$$f_{max} = \frac{10^9}{2\pi C |V| / (I_C - 1)} \qquad \text{EQ2-1}$$

For an IEPE accelerometer, there is a tradeoff between the maximum frequency (f_{max}) response versus the instantaneous voltage (a function of measured acceleration), where cable capacitance (C) and driving current (I_C) are constants. The expected sensor gain can be correlated to the sensor range (in g) and the voltage range (+/- 5V). Table 2-1 gives each module's sensor range, the approximate gains, and expected cable capacitance of planned lengths.

Table 2-1. Sensor and Cable Parameters

Sensor	Range (g)	Sensor Sensitivity (mV/g)	Cable Capacitance (pF)	Drive Current (mA)
Drift	50	100	36000	6
Drift	500	10	36000	6
Near-source	5000	1	36000	6

Assuming a constant driving voltage for an IEPE signal conditioner, a performance curve of the maximum frequency response of the system can be plotted against a peak instantaneous acceleration. The entire system's spectral response (sensor to accelerometer DAQ) was assumed to be limited by the DAQ sampling rates which were assumed to create an upper limit to performance (Figure 2-3). An imposed 40 kHz Nyquist frequency creates a pseudo-performance ceiling from a 80kHz DAQ sampling rate, although the sensor performance was expected to exceed the system ceiling at relatively low accelerations.

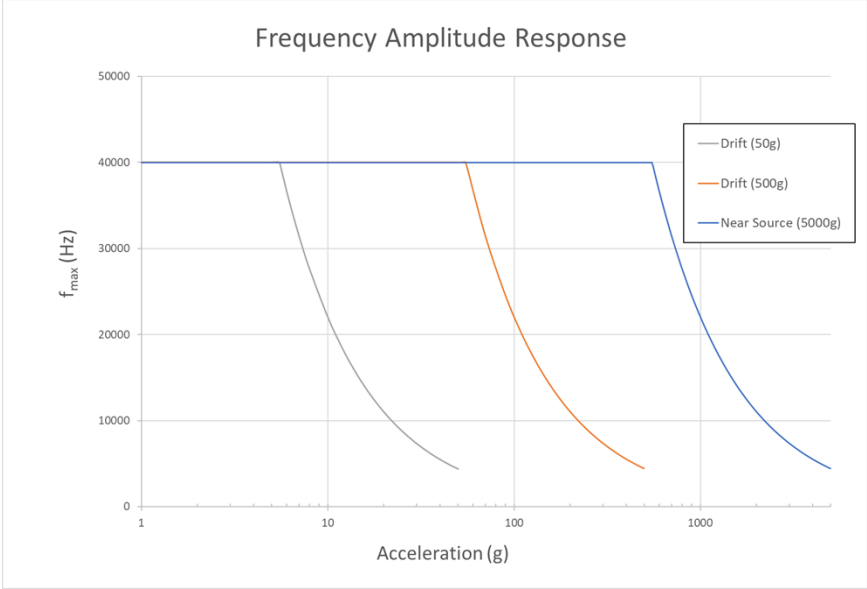

Figure 2-3. Expected frequency response of drift and near-source cables

2.6. Data Acquisition Facility

The 650 alcove was designed to house a large portion of the underground DAQ infrastructure by virtue of lowered ground motion as a function of distance from the source. It was located ~ 950 feet from the experiment and connected to the IEPE sensor modules by cables that could be up to 1200 ft. long. The accelerometer DAQ equipment included a Pacific Instruments (PI) 6000 series IEPE Acquisition System. Because our configuration used an analog sensor, we estimate accelerometer DAQ sensitivity as a function of digitizer resolution, accelerometer internal amplification and voltage range, which is shown in Table 2-2 as a function of nominally estimated sensitivity, a 16-bit digitization scheme and two possible accelerometer DAQ range values.

Table 2-2. DAQ and System Sensitivity

Sensor	Range (g)	Sensor Sensitivity (mV/g)	DAQ Digital Resolution (2^{bits})	DAQ Sensitivity (g) (+/- 5V range)	DAQ Sensitivity (g) (+/- 10V range)
Drift	50	100	65536	0.0015	0.0030
Drift	500	10	65536	0.0153	0.0306
Near-source	5000	1	65536	0.1526	0.3052

The 650 facility (see Section 3) also housed several 6029 PI IEPE amplifier-digitizer cards packaged into a 6000 series enclosure. The accelerometer DAQ system received a timing and firing pulse from a separate underground integrated data acquisition (IDAQ) network, which was run into a Stanford Delay Generator (SDG) to isolate potential noise on the trigger signal into the accelerometer DAQ. The IDAQ network developed by Pacific Northwest National Laboratory (PNNL) was not only used as a mechanism to distribute timing and firing signals, but also enabled data transfer and remote operation of the connected systems from outside the tunnel. Accelerometer DAQ components and the SDG were mounted into a rigid enclosure with cable breakout panels, a host computer with non-volatile storage and uninterruptable power sources. To prevent ground motion from damaging electronic components, wire-rope shock isolators were integrated into the feet of the rigid enclosure, which was mounted into the P-Tunnel infrastructure (Figure 2-4).

Figure 2-4. Accelerometer DAQ enclosure w/ shock isolators

3. INSTALLATION AND EMPLACEMENT

Key locations for the explosive chambers can be seen below in Figure 3-1. The first of the HE experiments; PE1-A in the northernmost part of P-Tunnel known as the U12p.06 drift. The DAQ infrastructure for the accelerometers was placed in the 650 Alcove, where ground motion was predicted to be orders-of-magnitude lower.

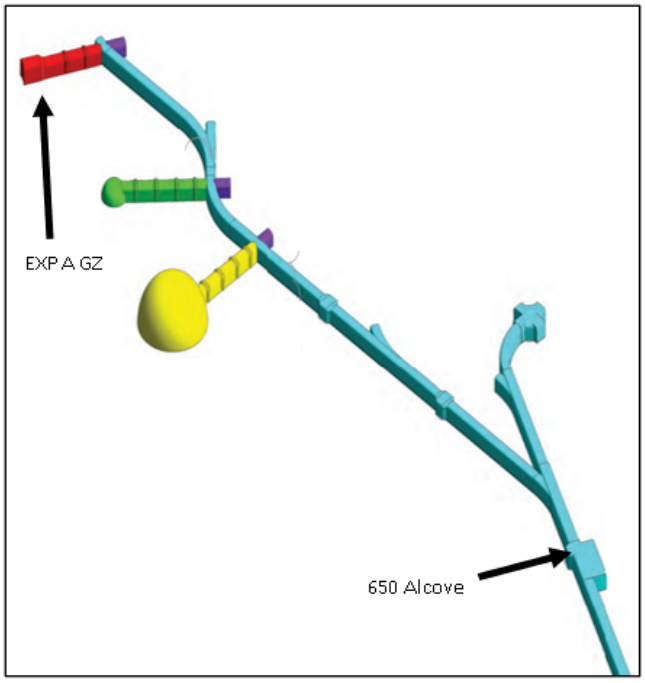

Figure 3-1. P-Tunnel infrastructure and experiment locations

Near-source module boreholes were drilled in the west rib of the tunnel at sub, super and horizontal inclinations, with conductor casing and closure flanges to support conveyance and grouting operations; drift module boreholes were drilled vertically into the invert (Figure 3-2).

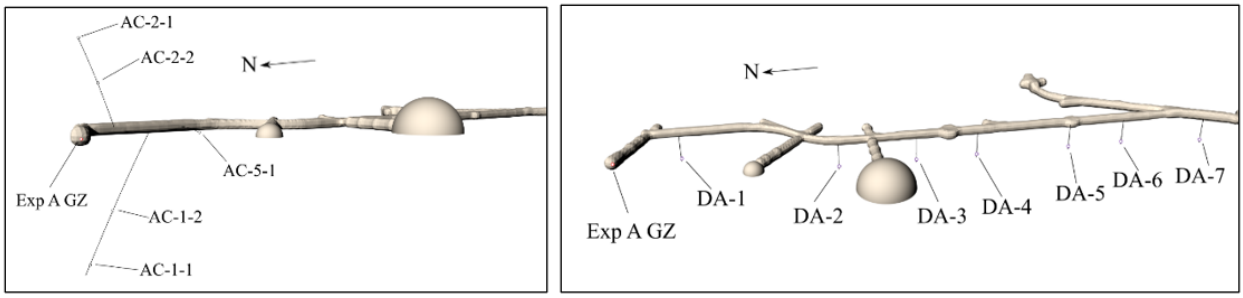

Figure 3-2. Instrument borehole locations
Near-source (left); Drift (right)

The accelerometer modules installed in sub-horizontal (AC-1, DA1-DA7) boreholes were conveyed along with a removable tremie tube, which was continuously pulled out of the open hole as it filled with grout. Instruments in super and horizontal boreholes (AC-2 and AC-5) were accommodated with one or more tremies and the grout was pumped in stages. In AC-2, grout was pumped through

the closure flange into a tremie that ran to the toe of the well where grout was gravity-forced back towards the flange. Air displaced by grout was allowed to return down the instrument's conveyance pipe, which was also run to the toe next to the nearest instrument (AC-2-1). Grout was pumped into the borehole to ensure annular instrument coverage in several stages, which was observed with a small borehole logging camera that imaged near-source instruments through clear PVC sections in the conveyance workstring. This same process served as a secondary verification of the instruments along the conveyance pipe, ensuring that they could be accurately logged at the desired depth in the boreholes.

Figure 3-3 shows examples of typical instrument mounting on semi-rigid PVC pipe (clear and opaque), including completed near-source rib mounted collars, and a grout-filled conductor casing of drift boreholes within a vault box installed into the tunnel invert.

Figure 3-3. Typical: Instruments emplaced in drift vaults and rib collars.
PVC pipe (left top: drift, bottom left: near-source), completed drift conductor within vault box (top right) and near-source conductor, collar (bottom left) and closure flange (bottom right)

In the final installation, we secured the instrumentation cable runs along the west rib (tunnel wall) towards the 650 facility, where the cables were passed under minecar rails and connected to the floor-mounted DAQ enclosure. Installation coordinates from GZ of the HE source are listed in Table 3-1.

Table 3-1. Emplaced Instrument Locations and Source Range

Instrument	Delta Easting (ft)	Delta Northing (ft)	Delta Elevation (ft)	Range (ft)	Range (m)	Scaled Range* ($m/kt^{1/3}$)
AC-1-1	10.27	4.71	109.25	109.83	33.47	132.01
AC-1-2	29.85	39.79	69.30	85.30	26.00	102.52
AC-2-1	3.17	3.03	-81.78	81.90	24.96	98.44
AC-2-2	35.23	34.98	-45.23	67.16	20.47	80.72
AC-5-1	-35.41	93.04	-3.53	99.62	30.36	119.73
DA-1	72.00	76.02	37.77	111.31	33.93	133.78
DA-2	12.14	280.81	38.32	283.67	86.46	340.95
DA-3	11.79	384.69	38.39	386.78	117.88	464.87
DA-4	11.49	468.80	38.86	470.55	143.42	565.56
DA-5	11.69	599.42	39.57	600.84	183.13	722.16
DA-6	11.76	676.54	39.48	677.79	206.58	814.64
DA-7	-3.26	788.08	39.95	789.10	240.51	948.43

* For 16.3 ton source

4. INSITU PERFORMANCE

4.1. Noise Assessment

To better account for the long cable lengths, we conducted a preliminary noise assessment to verify the performance of the entire accelerometer system that was installed in the underground. These assessments consisted of data collects during both quiet and highly active periods in the tunnel. For example, when ventilation off and no personnel activity, as well as periods of significant activity such as mining. Despite an incoming trigger, the typical zero offset or DC gain on the sensors was shown to have a noise floor ~ 0.1% of the full-scale signal of a 50 g & 500 g drift accelerometer, on all 148 channels (Figure 4-1, left). To evaluate the system's upper frequency performance and investigate any AC power coupling from the mine infrastructure, we used a spectral wavelet transform across all channels. Interrogation of the spectral content of the instrument waveforms during a quiet period in the tunnel illuminated the performance ceiling, which was expected to be > 5 kHz (Figure 4-1, right). Additionally, interrogation for 60 Hz AC power coupling into instrument cables or DAQ components was not present at substantial levels.

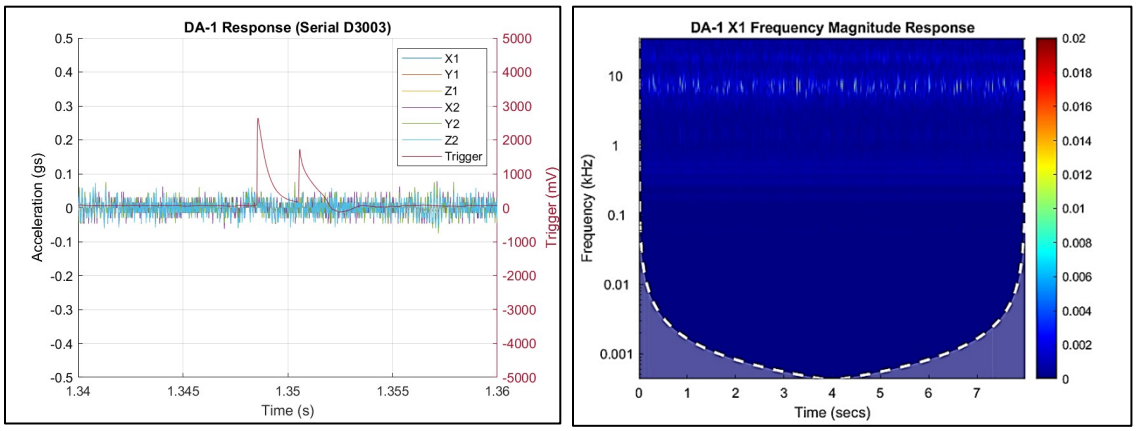

Figure 4-1. Initial drift accelerometer noise assessment;
Noise floor and trigger response (left); Wavelet transform with no excitation (right).

4.2. Dynamic Response Testing

Once the instrument network was assembled, the dynamic response of the system was evaluated using an accelerated weight drop (AWD) on the invert of the U12p.06 drift, creating vertical ground motion to elicit accelerometer response. Additionally, a series of strikes were conducted over the top of each drift vault at 1, 3, and 5 meter horizontal distances from the instruments locations. Due to the extremely weak ground motion, noise floor, and resolution, the near-source accelerometers were not able to resolve any excitation in either temporal or spectral analysis. The drift accelerometers' temporal and wavelet transform response to the AWD excitation was favorable and consistent across the drift accelerometer array; the 50 g orthogonal sets are shown as a typical example (Figure 4-2).

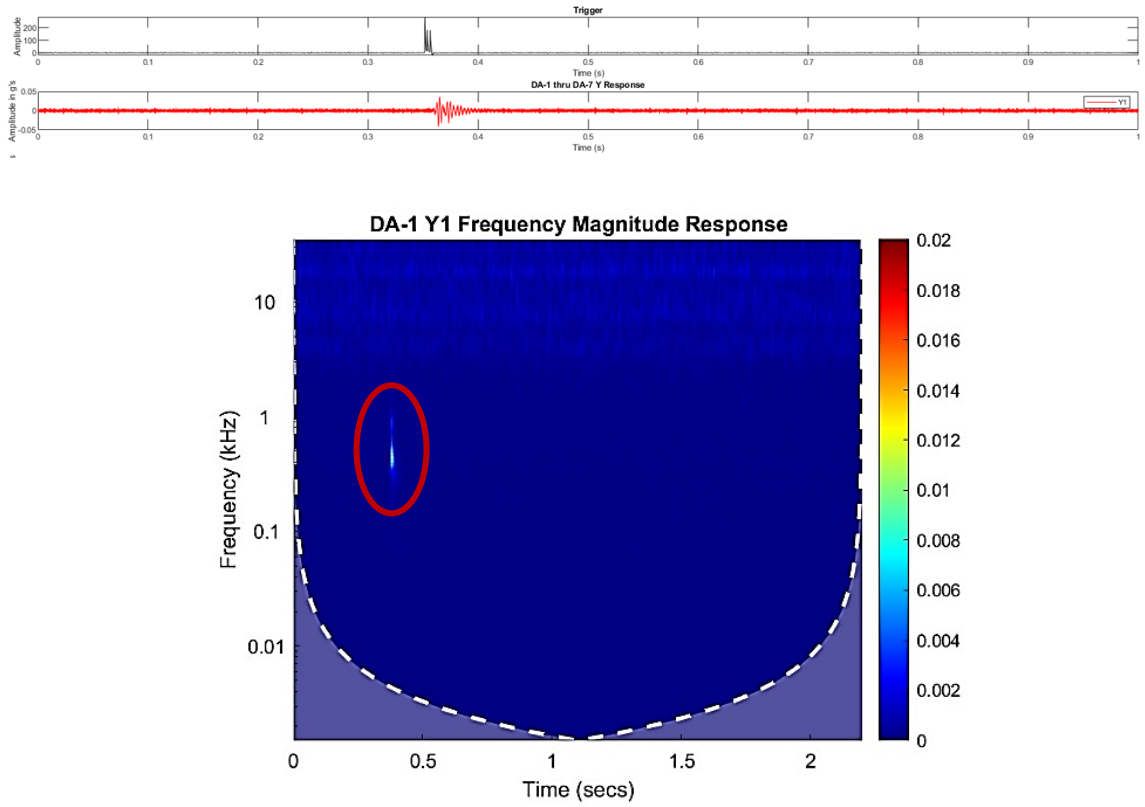

Figure 4-2. AWD drift accelerometer response
Temporal response(top) and seismic wavelet transform (bottom)

4.3. Experiment Performance

On October 18, 2023, the chemical HE source was detonated, resulting in full data collection on all 148 channels. Seismic signals were recorded on all accelerometer channels at 80 kHz and all IMU channels at 1 kHz. Only two channels experienced anomalous waveforms resulting in a 99% data return rate. An example of the near-field response is shown below in Figure 4-3.

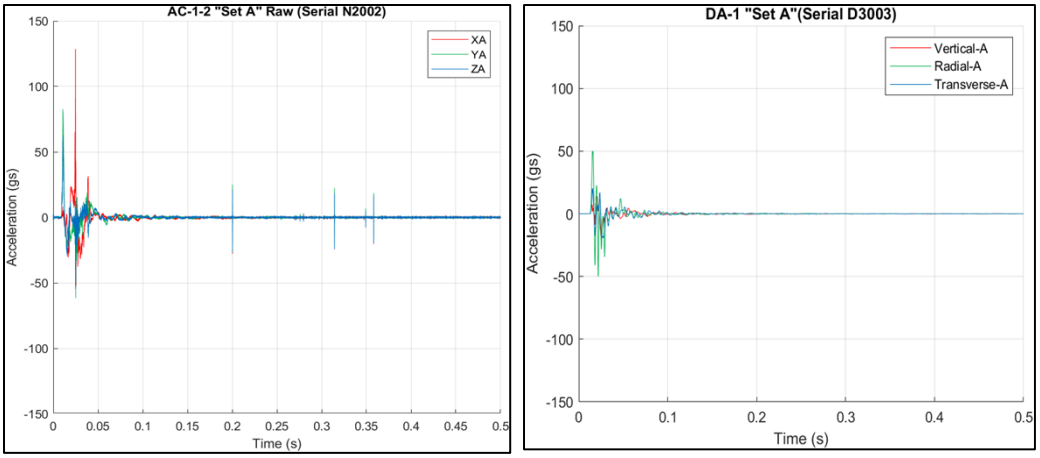

Figure 4-3. Raw waveform from near-source and drift accelerometers
AC-1-2 (left); DA-1 (right)

The further field accelerometers returned similar data quality, measuring accelerations close to 50 g in DA-1 for the radial direction (Figure 4-3, right) as amplitude decayed with increasing distance from the source. Ford (2020) predicts the transition to the linear (elastic) regime to start at approximately 150 m/kt$^{1/3}$ which starts somewhere between DA-1 and DA-2. Stacked radial waveform arrivals for the drifts are shown in Figure 4-4 showing reasonable transit times through undeformed rock. Changes in the waveform are observable across the drift array as high frequency components of the wave form are decrease along with the temporal amplitude as distance from the source increases.

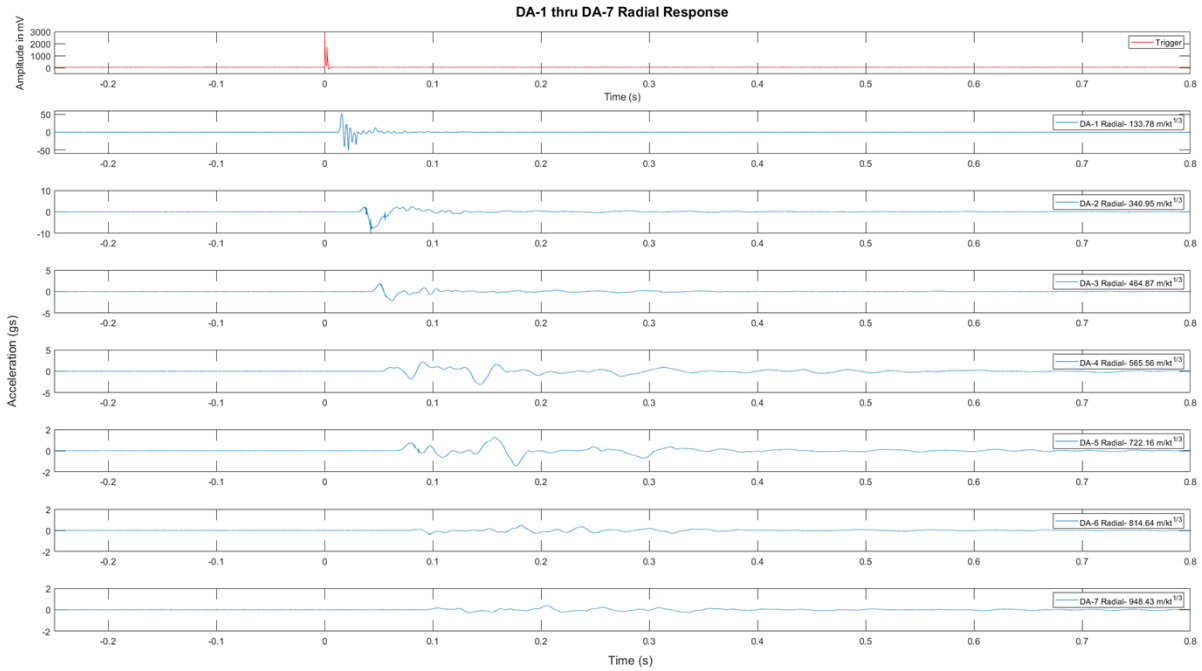

Figure 4-4. Radial waveform from drift accelerometers
Trigger (top) and DA-1 to DA-7 (second from top to bottom)

Immediately after the experiment, the accelerometer data acquisition system was reconfigured to collect data on remote triggering off the closest, high sensitivity DA-1 module at sensor responses

close to AWD amplitudes with the intention of capturing aftershocks. Data capture was triggered by a vertical ground motion threshold set by doubling the static noise floor of approximately 0.01 g with a sample rate of 2 kHz. Oversampling occurred with over 4,000 records being created by the accelerometer system over the course of several weeks.

Data exfiltration was accomplished remotely using the IDAQ, leading to data QC and minimal post processing before uploading into the LYNM PE1 data repository for use by the wider science community.

5. CONCLUSIONS

The first chemical explosive experiment (Experiment A) in the PE1 series successfully generated and collected prompt-free field ground motion data. Instruments designed and shock-tested for in-situ emplacement survived the experiment and continued to be responsive after the experiment was complete. Critical data was successfully acquired by the custom DAQ system, which was also successfully isolated from potentially damaging ground motion. The infrastructure installed for Experiment A will be repurposed for future experiments. Data from the experiments will be used to validate computational models to continue to advance our scientific understanding of signal propagation for underground explosions and, more specifically, how data from new experiments can be combined with legacy UGT data to better reveal how differences in sources influence near-field ground motion in volcanic tuff. Experience gained in this experiment will inform improvements to design and emplacement of instrumentation development for subsequent B and DL experiments.

REFERENCES

Bodmer, M., Townsend, M., Roberts, B., Wilson, J., Reppart, J., Smith, D., Downs, N., Feldman, J., Choens II, R. C., Heath, J., Holland, A., Barrow, P., Bartlett, T., Boukhalfa, H., Broome, S., Dietel, M., Downs, C., Ezzedine, S., Freimuth, C., Griego, J., Ingraham, M., Jaramillo, J., Jones, K., Kibikas, W., Kuhlman, K., Larotonda, J., Miller, A., Otto, S., Powell, M., Rodriguez, M., Tafoya, J., Valdez, N., Xu, G., and Lyons, S. "LYNM PE1 Pre-Experiment A Site Characterization Report." Technical Report SAND2024-07522. Sandia National Laboratories, Albuquerque, New Mexico, June 2024.

Denny, M. D., and Stull, S. P. "Proceedings of the Symposium on the Non-Proliferation Experiment (NPE): Results and Implications for Test Ban Treaties." United States: N. p., 1994. Web.

Erskine, D., W. J. Nellis, and S. T. Weir. "Shock Wave Profile Study of Tuff from the Nevada Test Site." Journal of Geophysical Research 99, no. B8 (1994): 15529–15537. doi:10.1029/94JB00726.

Fourney, W. L., Dick, R. D., Taylor, S. R., and Weaver, T. A. "An Analysis of Three Nuclear Events in P-Tunnel." United States: N. p., 1994. Web. doi:10.2172/10156509.

Ford, S. R. "Free-Field Ground Motion Induced by Underground Explosions at Aqueduct Mesa with Predictions for Physical Experiment One (PE1)." United States: N. p., 2020. Web. doi:10.2172/1605054.

Goldstein, P., and Jarpe, P. S. "Comparison of Chemical and Nuclear Explosion Source-Time Functions from Close-In, Local, and Regional Seismic Data." Arms Control and Nonproliferation Technologies, 1994. DOE/AN/ACNT-94A.

Larotonda, Jennifer M., and Townsend, Margaret J. "Data Release Report for the Source Physics Experiment Phase II: Dry Alluvium Geology Experiments (DAG-1 through DAG-4)." Nevada National Security Site. United States: N. p., 2021. Web.

Mellors, Robert, Abbott, Robert, Steedman, David, Podrasky, David, and Pitarka, Arben. "Modeling Subsurface Explosions Recorded on a Distributed Fiber Optic Sensor." Journal of Geophysical Research: Solid Earth 126 (2021). doi:10.1029/2021JB022690.

Myers, S. C., G. Abbott, T. Alexander, E. Alger, A. Alvarez, A. Navarro, T. Antoun, G. Auld, A. Malach, H. Banuelos, M. Barela, T. Barnhart, P. Barrow, T. Bartlett, A. Bockman, M. Bodmer, K. Bogolub, J. Bonner, R. Borden, H. Boukhalfa, D. Bowman, C. Britt, B. Broman, S. Broome, B. Brown, J. Burghardt, D. Chester, C. Choens, K. Chojnicki, A. Churby, J. Cole, T. Coleman, J. Collard, A. Couture, G. Crosby, A. Cruz-Cabrera, D. D'Saint Angelo, D. Musa, W. Dekin, B. DeVisser, M. Dietel, C. Downs, N. Downs, E. Dzenitis, E. Eckert, S. Eras, G. Euler, S. Ezzedine, J. Fast, J. Feldman, K. Featherston, M. Foxe, C. Freimuth, B. Fritz, G. Galvin, S. Gamboa, L. Garner, T. Gascoigne, J. Gastelum, et al. "A Multi-Physics Experiment for Low-Yield Nuclear Explosion Monitoring." 17p. 2024.

Smith, C. "Gage Cookbook: Tools and Techniques to Measure Stresses and Motions on Explosive Experiments." Technical Report SAND 96-0200. Sandia Laboratories, Albuquerque, New Mexico, January 1996.

Townsend, Margaret, Obi, Curtis, Abbott, Robert, Bowman, Daniel, Mellors, Robert, Wharton, Sonia, Schalk, Walter, Smith, Ken, Plank, Gabe, Steedman, David, and Walter, William. "Data Release Report Source Physics Experiments 5 and 6 (SPE-5 and SPE-6)." Nevada National Security Site. United States: N. p., 2019. Web. doi:10.2172/1525892.

Rougier, E., and H. J. Patton. "Seismic Source Functions from Free-Field Ground Motions Recorded on SPE: Implications for Source Models of Small, Shallow Explosions." Journal of Geophysical Research: Solid Earth 120 (2015): 3459–3478. doi:10.1002/2014JB011773.

DISTRIBUTION

Email—Internal

Name	Org.	Sandia Email Address
Giorgia Bettin	8916	gbettin@sandia.gov
Scott Broome	8914	stbroome@sandia.gov
Jose Falliner	6752	jlfalli@sandia.gov
Leiph Preston	8911	lpresto@sandia.gov
Steve Vigil	6756	srvigil@sandia.gov
Lauren Wheeler	8913	lwheele@sandia.gov
Technical Library	1911	sanddocs@sandia.gov

Email—External

Name	Company Email Address	Company Name
John Lazarz	John.lazarz@nnsa.doe.gov	NA-22
Sean Ford	ford17@llnl.gov	LLNL
Hunter Knox	hunter.knox@pnnl.gov	PNNL
Chris Strickland	christopher.strickland@pnnl.gov	PNNL
Bill Walter	walter5@llnl.gov	LLNL

This page left blank.

This page left blank.

Sandia National Laboratories

Sandia National Laboratories is a multimission laboratory managed and operated by National Technology & Engineering Solutions of Sandia LLC, a wholly owned subsidiary of Honeywell International Inc. for the U.S. Department of Energy's National Nuclear Security Administration under contract DE-NA0003525.